OXFORD

Cerebral Cortex, 2023, **33**, 9822–9834
https://doi.org/10.1093/cercor/bhad247
Advance access publication date 6 July 2023
Original Article

Function and biochemistry of the dorsolateral prefrontal cortex during placebo analgesia: how the certainty of prior experiences shapes endogenous pain relief

Lewis S. Crawford [1], Emily P. Mills[1], A. Peek[1], Vaughan G. Macefield[2], Kevin A. Keay[1], Luke A. Henderson [1,*]

[1]School of Medical Sciences (Neuroscience), Brain and Mind Centre, University of Sydney, Sydney 2006, Australia,
[2]Department of Neuroscience, Monash University, Clayton, VIC 3800, Australia

*Corresponding author: Department of Anatomy and Histology, F13, University of Sydney, Sydney 2006, Australia. Email: lukeh@anatomy.usyd.edu.au

Prior experiences, conditioning cues, and expectations of improvement are essential for placebo analgesia expression. The dorsolateral prefrontal cortex is considered a key region for converting these factors into placebo responses. Since dorsolateral prefrontal cortex neuromodulation can attenuate or amplify placebo, we sought to investigate dorsolateral prefrontal cortex biochemistry and function in 38 healthy individuals during placebo analgesia. After conditioning participants to expect pain relief from a placebo "lidocaine" cream, we collected baseline magnetic resonance spectroscopy (^{1}H-MRS) at 7 Tesla over the right dorsolateral prefrontal cortex. Following this, functional magnetic resonance imaging scans were collected during which identical noxious heat stimuli were delivered to the control and placebo-treated forearm sites. There was no significant difference in the concentration of gamma-aminobutyric acid, glutamate, Myo-inositol, or N-acetylaspartate at the level of the right dorsolateral prefrontal cortex between placebo responders and nonresponders. However, we identified a significant inverse relationship between the excitatory neurotransmitter glutamate and pain rating variability during conditioning. Moreover, we found placebo-related activation within the right dorsolateral prefrontal cortex and altered functional magnetic resonance imaging coupling between the dorsolateral prefrontal cortex and the midbrain periaqueductal gray, which also correlated with dorsolateral prefrontal cortex glutamate. These data suggest that the dorsolateral prefrontal cortex formulates stimulus–response relationships during conditioning, which are then translated to altered cortico-brainstem functional relationships and placebo analgesia expression.

Key words: placebo analgesia; dorsolateral prefrontal cortex; acute pain; conditioning; variability.

Introduction

Placebo effects, where the administration of an inactive substance leads to physiological benefit, or indeed, where the administration of a pharmacologically active substance produces benefit beyond its attributable properties, are grounded in an individual's prior experiences and their expectations of improvement (Amanzio and Benedetti 1999; Büchel et al. 2014; Medoff and Colloca 2015; Ashar et al. 2017). In the context of pain, the phenomenon of placebo analgesia has been extensively studied and associated with a number of factors including conditioning effectiveness, participant–experimenter interactions, and value statements (Colloca and Benedetti 2006; Kaptchuk et al. 2009; Kong et al. 2009; Colloca et al. 2010; Colloca 2019). Together, these factors inform a participant's expectations of how effectively a treatment—unbeknownst to them, a placebo—will work to reduce their pain—that is, their precision.

It has been hypothesized that the midbrain periaqueductal gray (PAG)—rostral ventromedial medulla—dorsal horn brainstem circuit mediates placebo analgesia and we recently used ultrahigh-resolution functional magnetic resonance imaging (fMRI) to show that placebo analgesic responses are indeed associated with activity changes in this circuit (Crawford et al. 2021). Given that placebo analgesia requires complex cognitive function to integrate prior experiences and expectations with incoming nociceptive events, it is likely that PAG activity and ultimately placebo analgesia is driven by descending inputs from higher-order cortical regions. Consistent with this idea, human brain imaging studies have revealed that activity changes in the dorsolateral prefrontal cortex (dlPFC) are associated with placebo analgesia in addition to expectations, decision-making, and error-prediction (Wager et al. 2004; Rosenbloom et al. 2012; Schenk and Colloca 2020; Hibi et al. 2020).

Furthermore, experimental manipulation of dlPFC function can either attenuate or amplify placebo analgesia. For instance, Krummenacher et al. (2010) demonstrated in an expectation-based placebo pain paradigm that transient disruption of the dlPFC through repetitive transcranial magnetic stimulation blocked the generation of placebo analgesia. This same intervention, however, had no effect on the sensory experience of pain itself. Conversely, Tu et al. (2021) used transient direct current stimulation (tDCS) to demonstrate that compared with sham stimulation, cathodal tDCS applied to the right dlPFC increased placebo analgesic response magnitudes and altered dlPFC functional connectivity. Given these

Received: April 5, 2023. **Revised:** June 15, 2023. **Accepted:** June 17, 2023

findings, it is likely that the PAG is driven by inputs from the dlPFC either directly or via a relay in the rostral anterior cingulate cortex (rACC; Eippert et al. 2009; Sevel et al. 2015).

It has also been recently proposed that brainstem pain modulatory circuits are governed by a Bayesian system in which prior experiences are integrated with incoming nociceptive information to form the pain percept and subsequent placebo analgesia. Grahl et al. (2018) applied a Bayesian model over 2 groups of participants. One group experienced a highly precise conditioning paradigm whereby they received identical low noxious stimuli (to generate consistent expectations of analgesia), and the other group experienced a low precision conditioning paradigm in which they received highly variable noxious stimuli (to generate variable expectations of analgesia). High conditioning precision (leading to consistent expectations of low pain) was associated with greater placebo analgesia, and changes in PAG activation reflected how effectively a participant was able to combine their current pain experience with their prior experiences and expectations for pain reduction to elicit placebo analgesia. Indeed, while it is possible to separately investigate the effects of expectations and conditioning on the generation of placebo analgesia (Amanzio and Benedetti 1999), the 2 are often intermingled, and their effects are additive in nature. It is difficult to explain the effects of conditioning without conceding that these procedures likely create expectations—either positive or negative—toward the inert treatment. Similarly, even when expectations are generated without employing an experimental conditioning model, an argument can be made that an individual's prior experiences, contextual cues, and participant–experimenter interactions play an analogous role to conditioning signals.

The Bayesian brain model accounts for the additivity of these 2 factors, suggesting that fluctuations in conditioning effectiveness may influence the strength of expected relief from a placebo, capturing the duality of these 2 factors. However, since both chronic pain sufferers and pain-free participants show spontaneous fluctuations in perceived pain either over time (in the case of chronic pain; Parry et al. 2017; Mills et al. 2020), or in response to a series of identical acute noxious stimuli (in those that are pain free; Henderson et al. 2020; Crawford et al. 2022), it is possible that inherent differences in the ability to consistently perceive pain may underlie an individual's ability to mount Bayesian-based phenomena such as placebo analgesia.

The current study aimed to investigate: (i) whether low variability in pain intensity ratings during conditioning phase (high conditioning pain rating consistency) is associated with stronger placebo responses and (ii) whether dlPFC biochemistry, function, and functional connectivity are associated with placebo responsiveness and conditioning pain rating consistency. Previously, we demonstrated that dlPFC signal intensity changes were strongly associated with variability of perceived pain intensity during a set of identical noxious stimuli (Crawford et al. 2022). Given this, we propose that decreased pain intensity variability during identical noxious stimuli (conditioning pain rating consistency) would be associated with increased magnitude of placebo responses as well as altered function of the dlPFC and its connections to the PAG. Additionally, we hypothesized that placebo responders would demonstrate greater consistency in pain rating responses during conditioning and that this consistency, as well as reported reductions in pain (placebo responses), would relate directly to both functional connectivity differences and biochemistry in the dlPFC.

Materials and methods

Ethics

All experimental procedures were approved by the University of Sydney Human Research and Ethics Committee (HREC number 2019/037) and were consistent with the Declaration of Helsinki. Participants provided written informed consent prior to experimental proceedings. While inside the MRI scanner, participants were supplied with an emergency button and instructed to squeeze the button to stop the experiment at any time. After all testing, participants were informed verbally and through a written statement of the necessary deception within the experiment and invited to seek any additional clarification of what they had experienced. The data were collected as part of a larger study, some of which has already been published (Crawford et al. 2021).

Participants

Thirty-eight healthy control participants were recruited for the study (18 females; mean ± SEM age 25.0 ± 0.8 years; range 20–37 years). An a priori power analysis using a previous brain imaging study investigating interactions between positive expectations and pain relief (Grahl et al. 2018) revealed that a total sample size of 34 would be necessary to detect similar neural effects with 90% power (d = 0.46, α = 0.05, power = 0.90; Faul et al. 2007).

Experimental design

The study involved 3 independent sessions conducted over 2 successive days: *Conditioning* (*day* 1), *Reinforcement* (*day* 2), and *Test* (*day* 2; Fig. 1A). Throughout all 3 sessions, noxious thermal stimuli were administered using a 3 × 3 cm Peltier-element thermode (TSA-II, Medoc) applied to the left or right arms, onto sites where 2 different creams were applied, a *control* (Vaseline) or *placebo* (lidocaine) cream. In all 3 sessions, these creams were removed from participant's forearms by carefully wiping the skin surface with an alcohol swap directly before applying thermal noxious stimuli. Each stimulus lasted a total of 15 s, including a ramp up from baseline (32°C), a plateau at the designated noxious temperature (low or moderate, depending on cream site), and a ramp down to baseline. Each stimulus period was separated by a 15-s inter-trial interval at the baseline 32°C temperature. Outside the scanner (sessions 1 and 2) participants rated their pain continuously using a computerized visual analog scale (VAS). Inside the scanner (session 3), the VAS was replicated onto a digital screen overhead and participants continually reported their pain throughout scanning by controlling a slider on this screen using a 2-button button box with their left index finger (100 = worst pain imaginable; 0 = no pain).

Day 1—conditioning

Prior to conditioning, thermal thresholds were assessed and participants were presented with the control and placebo creams. A determination of moderate pain protocol was conducted where 0.5°C interval temperatures between 44 and 48.5°C were randomly applied sequentially to participant's left volar forearm. Participants were informed that 1 temperature was being recorded: a moderate temperature that elicited a VAS pain rating between 40 and 50, which would then be applied to both cream sites throughout the remainder of the experiment. In reality, we recorded 2 temperatures: a low temperature (one which elicited a 20–30 VAS rating) as well as the moderate temperature (40–50 VAS).

The 2 creams were then applied to participant's right forearm. Despite both creams being identical, the verbal description

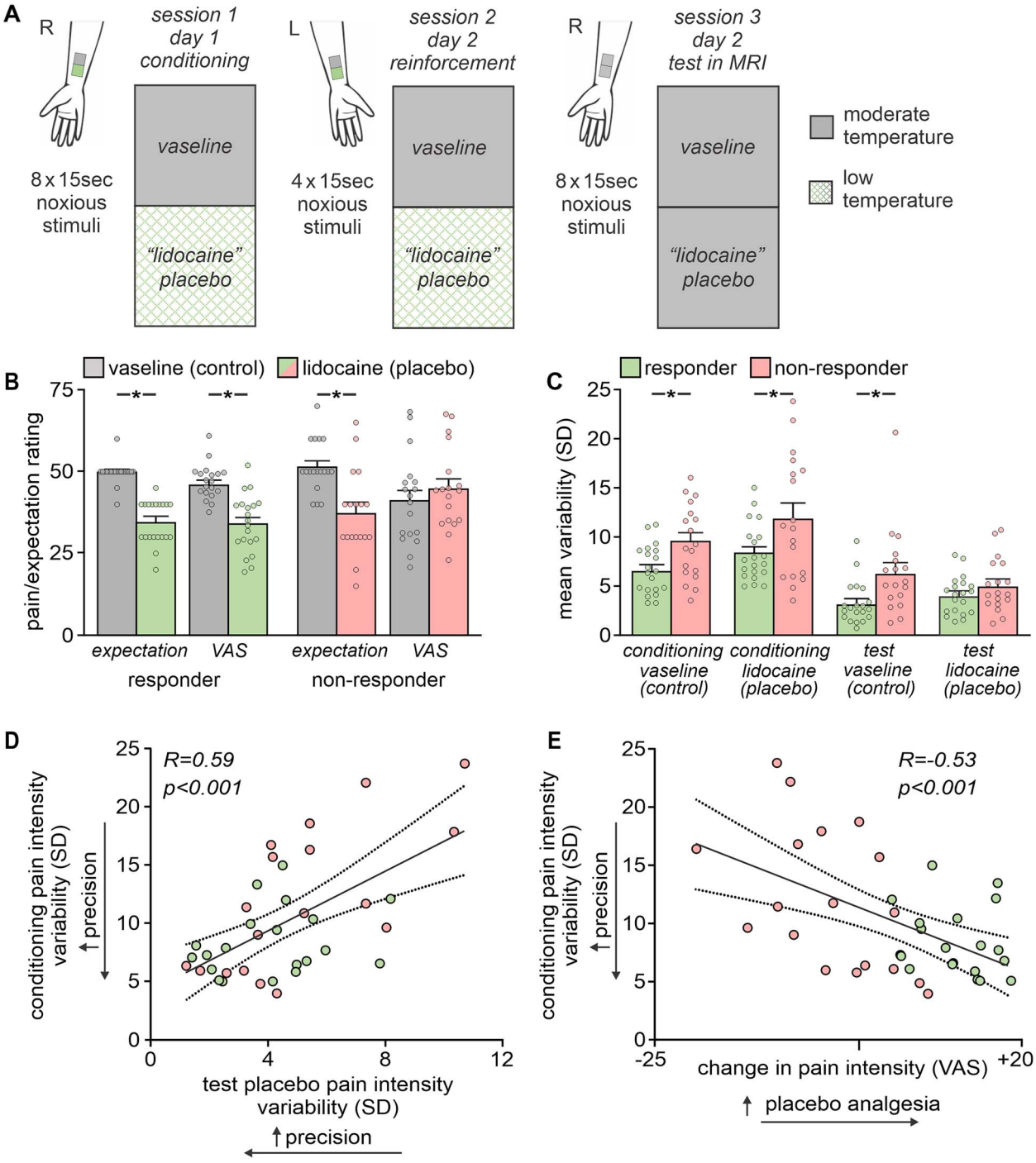

Fig. 1. Experimental methodology and psychophysics. A) During conditioning and reinforcement phases, lower intensity noxious thermal stimuli were deceptively applied to the placebo "lidocaine" cream site relative to a control Vaseline cream. In the test phase, while collecting functional MRI, the 2 cream sites received identical moderate intensity noxious stimuli sequentially (i.e. scan 1 = stimulation of the Vaseline control site, scan 2 = stimulation of the placebo "lidocaine" site). B) Plots of mean ± SEM expected and actual pain intensity ratings in responder and NR groups. Despite not demonstrating a placebo response, NR expected significant pain relief via administration of the placebo "lidocaine" cream directly prior to the application of test phase stimuli. $^*P < 0.001$. C) Plots of mean ± SEM pain intensity variability (SD) during conditioning and test. Placebo NR demonstrated significantly greater variability in their pain ratings during conditioning, which continued during the test phase inside the scanner when the control Vaseline cream site was stimulated. $^*P < 0.001$. D) Plot of pain rating variability during the stimulation of the placebo "lidocaine" cream during the test phase against variability during the stimulation of the placebo "lidocaine" cream during the preceding conditioning phase. Note that pain percept precision displays intraindividual consistency between experimental phases occurring over 2 subsequent days. The solid line indicates the regression slope between these variables, with dotted lines the upper and lower 95% confidence interval of this slope. E) Plot of pain rating variability during the conditioning phase stimulation of the placebo "lidocaine" site against the magnitude of placebo analgesia generated in the test phase. That is, the lower the variability in participant's pain ratings during placebo conditioning, the greater a placebo analgesic response they generated on the following day. The solid line indicates the regression slope of these variables, with dotted lines the upper and lower 95% confidence interval of this slope.

given, and physical appearance of the control and placebo creams differed to elicit initial expectations of analgesic properties. The control cream bottle appeared white, with a label stating it was a Vaseline solution and no coloring additives were added to this cream. In contrast, the placebo cream bottle appeared green, with a label stating it was a "Lidocaine" solution. Green food coloring was also added to this cream and it was described to hold analgesic properties, which could reduce the thermal sensitivity in a localized region. The 2 creams were then applied in a counterbalanced fashion to proximal and distal sites on volar aspect of the forearm overlapping with the C6 dermatome.

Following this procedure, 2 rounds of conditioning were conducted on the respective cream sites. Each round of conditioning involved a series of 8 noxious stimuli being applied to each of the cream sites. Participants were informed that both creams were receiving *identical* noxious stimuli at the temperature previously eliciting a moderate pain intensity during the determination procedure. In reality, we applied the *low* temperature to the placebo "Lidocaine" cream site, and the *moderate* temperature only to the control Vaseline site. Prior to each series of stimuli, participants were asked to report their average expected pain across the 8 stimuli and reported their pain throughout using the computerized VAS. After a total of 16 stimuli had been applied to each cream site, participants were asked to return the following day at an identical time to conduct the scanning component of the experiment.

Day 2—reinforcement and test

Upon return, both the control Vaseline and placebo "lidocaine" creams were applied in the same counterbalanced locations to participant's left and right volar forearms. Reinforcement was conducted inside the MRI scanner room with participants laying supine on the scanner bed, and noxious stimuli were applied to the left volar forearm to reduce the likelihood of sensitization effects on the right forearm. Reinforcement involved a series of 4 noxious stimuli being applied to both cream sites at the same moderate and low temperatures as in conditioning to ensure that despite the change of day and immediate environment, participants continued to both expect and experience different pain responses between the control and placebo creams, respectively (Fig. 1A).

Following reinforcement, structural brain scans including a T1-weighted anatomical and magnetic resonance spectroscopy (^{1}H-MRS) scan were collected prior to the test phase. Unlike conditioning and reinforcement, the test phase involved identical moderate intensity stimuli being applied to *both* the control Vaseline and placebo "lidocaine" cream sites on the right volar forearm. Each cream site received 8 noxious stimuli, during which functional brain scans (fMRI) were collected. During both the reinforcement and test phases, participants continued to report their average expected pain prior to each series of noxious stimuli, as well as rate their pain continuously using the VAS systems.

Imaging protocol

Brain images were collected with a whole-body Siemens MAGNETOM 7T MRI system with a combined single-channel transmit and 32-channel receive head coil (Nova Medical). Participants were positioned supine on the scanner bed with support to minimize head movement. Prior to the test protocol, a T1-weighted anatomical image set covering the whole brain was acquired (repetition time = 5,000 ms, echo time = 3.1 ms, flip angle 1 = 4°, flip angle 2 = 5°, raw voxel size = 0.73 × 0.73 × 0.73 mm, 224 sagittal slices, scan time = 7 min). Immediately following this acquisition, the siemens standard automated shimming procedure (repetition time = 8,500 ms, echo time = 6 ms, flip angle = 90°) and a single voxel ^{1}H-MRS was acquired using a Stimulated Echo Acquisition Mode (STEAM) sequence (32 averages, spectral width = 6,000 Hz, water suppression = standard, reference amplitude = 215 V, mixing time = 32 ms, scan time = 5 min 06 s) encompassing a 20 × 20 × 20 mm voxel overlying the right dlPFC (Mylius et al. 2013). In all participants, the dlPFC MRS cube was bordered laterally by the skull wall, superiorly by the superior frontal sulcus, and inferiorly by the inferior frontal sulcus (Fig. 2B). The 2 fMRI sequences each consisted of a series of 134 gradient-echo echo-planar, using blood oxygen level-dependent (BOLD) contrast covering the entire brain. Images were acquired interleaved with a multiband factor of 4 and an acceleration factor of 3 (repetition time = 2,500 ms, echo time = 26 ms, raw voxel size = 1.0 × 1.0 × 1.2 mm, 124 axial slices, scan time = 6 min 25 s).

Imaging preprocessing and statistical analyses were performed using statistical parametric mapping (SPM12; Penny et al. 2011) and custom software. Each participant's raw dlPFC ^{1}H-MRS spectroscopy was first inspected to ensure data quality and maximal Cramer–Rao Lower Bounds (CRLB) values for gamma-aminobutyric acid (GABA), glutamate (Glu), Myo-inositol (mINS), and N-acetylaspartate (NAA) were 19, 2, 3, and 2%, respectively. Additionally, the full width at half maximum (FWHM) distribution of the spectra across all 36 participants did not exceed the established rejection cutoff of 21 Hz (mean ± SEM FWHM 9.63 ± 0.25 Hz). ^{1}H-MRS metabolite concentrations were quantified using LCModel version 6.3-1N (Provencher 1993) operated within the custom GUI provided by Osprey version 2.0.0 (Oeltzschner et al. 2020). A raw 7-T STEAM basis set was loaded and parsed into LCModel to create outputs of estimated concentration (mmol.L^{-1}) and CRLB; standard deviations (SD) expressed as a percent of the estimated concentrations. The Gannet Co-Register and Gannet Segment modules were utilized within Osprey, calling SPM12 to determine the tissue volume fractions of gray matter, white matter, and cerebrospinal fluid (CSF). Gannet Quantify then returns relative metabolite levels in institutional units, corrected for effects of tissue water content and relaxation effects (Harris et al. 2015). Metabolites of interest included Glu and GABA: the central nervous system's primary excitatory and inhibitory neurotransmitters, which play a broad role in emotional and cognitive processing of pain, as well as signaling memory formation and retrieval (Hassel and Dingledine 2012; Peek et al. 2020). Additionally, because of their role in pain processing, we also assessed mINS and NAA for group-level differences. Reduced concentrations of both mINS and NAA have been associated with chronic pain disorders and suggested to contribute to deficiencies in pain processing (Grachev et al. 2000, 2002; Gussew et al. 2011).

Functional image series were slice-timing corrected, motion corrected, and the resulting 6 directional movement parameters inspected to ensure that neither 1 mm of linear movement nor 0.5° of rotational movement was exceeded in any direction. Images were then linearly detrended to remove global signal changes, and the DRIFTER toolbox was used to remove physiological noise associated with cardiac and respiratory frequencies and harmonics (Särkkä et al. 2012). Signal change relating to the 6 movement parameters previously extracted was modeled and removed using a linear modeling of realignment parameters procedure. Each individual's 2 fMRI image series were then co-registered to their own T1-weighted anatomical image, and the T1 was spatially normalized to the DARTEL template in Montreal Neurological Institute (MNI) space. These normalization

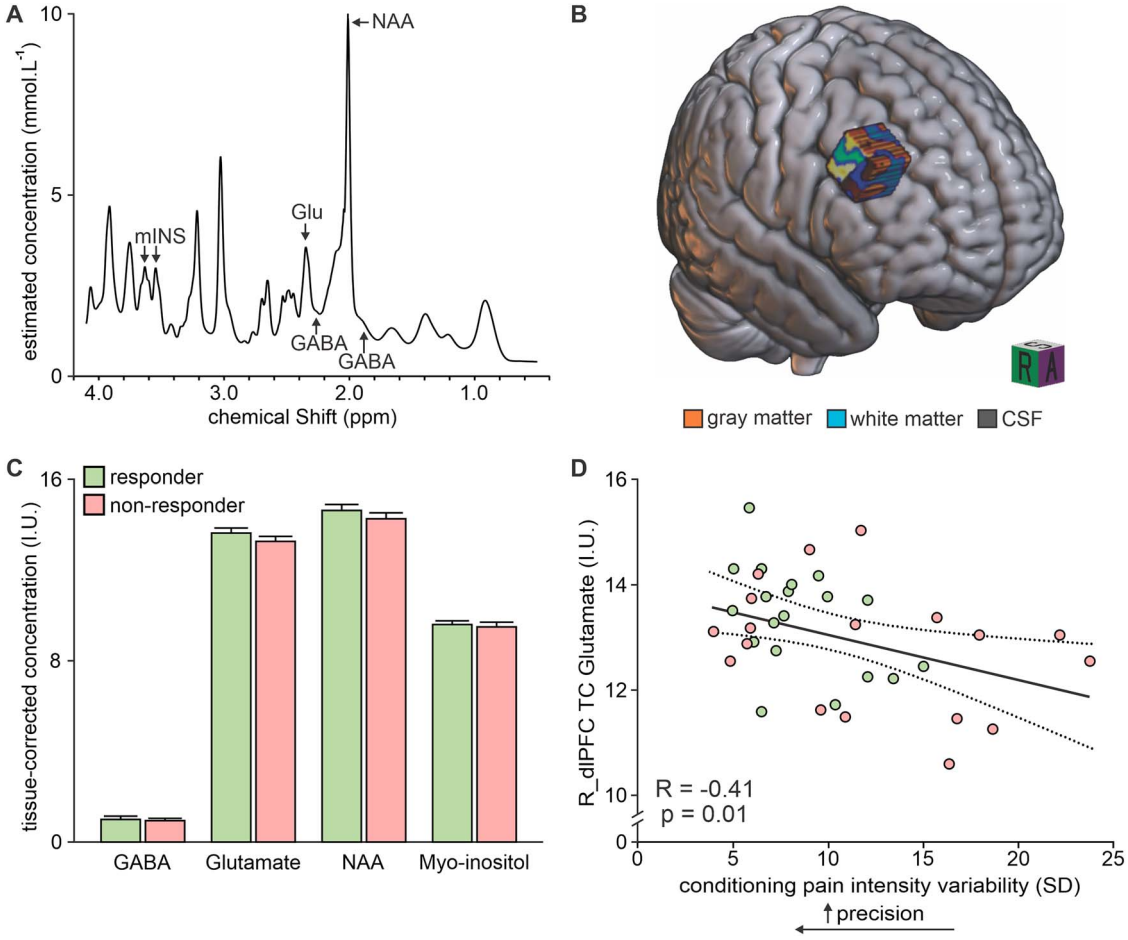

Fig. 2. Biochemical metabolite concentrations within the right dlPFC. A) An example trace of metabolite concentrations as resolved through the LCModel spectroscopy processing pipeline; B) location of the mean cube placed over the right dlPFC overlaid onto a rendered view of a T1-weighted anatomical image. Different colors indicate tissue composition; C) mean tissue-corrected concentration of key metabolites within the right dlPFC in responders and NR. We identified no group-level differences in GABA, Glu, NAA, or mINS; D) plot of tissue-corrected concentration of Glu and pain intensity rating variability (precision) during application of low intensity noxious stimuli to the placebo-treated site during conditioning. TC, tissue corrected.

parameters were then applied to the fMRI images to ensure each image series between participants occupied an identical template space. Normalized fMRI images were then spatially smoothed using a 6 mm FWHM Gaussian filter.

After revealing a cluster within the midbrain PAG in initial analyses, the spatially unbiased infratentorial template (SUIT) toolbox image segmentation and normalization pipelines were conducted, resulting in the brainstem and cerebellum of each participant being isolated in T1 and fMRI image series (Diedrichsen 2006). During this process, raw images were resliced to 0.5 mm isotropic voxels, and spatially smoothed using a 1 mm FWHM Gaussian filter to enable better spatial localization and parameter estimate extraction from this specific cluster.

Determining placebo responses

Each participant was classified as either a placebo responder or nonresponder (NR) based on the 2 SD band technique employed previously in investigating functional brain changes related to pain modulatory phenomena (Youssef et al. 2016; Crawford et al. 2021). During the test phase, the mean and SD of perceived pain intensities during each stimulation period were calculated for both the control Vaseline cream series and the placebo "lidocaine" cream series. If the mean pain intensity during the placebo series was more than 2 SD lower than the mean control pain intensity, the participant was considered to be a placebo responder.

Statistical analyses

All behavioral and extracted imaging data analysis was performed in Graphpad Prism version 9.5.1 (Swift 1997). First, the temperature of noxious stimuli elected as moderately painful in both placebo responders and NR was inspected to ensure that the magnitude of placebo analgesia generated did not relate to the degree of sensory input. Next, differences in both expected and perceived pain intensity magnitude changes, variability during both the conditioning and test phases, as well as metabolite concentrations within the right dlPFC, specifically GABA, Glu, mINS, and NAA, were compared between placebo responders and NR using 2-sample *t*-tests (2-tailed, $P < 0.05$). Additionally, linear regression analyses were conducted between pain intensity changes, pain intensity variability, and the concentrations of each of these pain-related metabolites (Pearson's correlations, $P < 0.05$ corrected for multiple comparisons).

Changes in signal intensity during the fMRI scans were determined using a repeated boxcar model convolved with a hemodynamic delay function where "1" was entered for the noxious stimulation periods and "0" for the baseline and interstimulus interval periods. The resultant brain contrast maps were then entered

into second-level random effects analyses to determine the main effect of pain (pain > baseline/pain < baseline) and the main effect of placebo (placebo > pain/placebo < pain). A threshold of $P < 0.05$, family-wise error corrected for multiple comparisons was applied to both analyses. Since no voxels survived this stringent threshold for the main effect of placebo analysis, the threshold was set at $P < 0.001$ uncorrected for multiple comparisons. To reduce the likelihood of type II errors, a cluster extent threshold of 20 contiguous voxels was applied to both functional analyses and small volume correction was performed on each cluster using individual parcels from the human connectome project extended (HCPex) atlas (Woo et al. 2014; Huang et al. 2022).

In addition, a significant cluster within the right dlPFC resulting from the main effect of placebo analysis was used as a seed region for conducting a whole-brain, voxel-by-voxel functional connectivity analysis over each of the fMRI scans in the placebo responder group. The location of this dlPFC seed overlapped with the dlPFC ^{1}H-MRS voxel. These whole scan functional connectivity contrast images were then entered into second-level random effects analysis and a main effect of placebo assessed in the placebo responder group. The results were displayed at $P < 0.001$, uncorrected for multiple comparisons, and each cluster was then subject to, and survived small volume correction ($P < 0.05$). These clusters were then saved as volume-of-interest masks and connectivity values extracted to determine differences between "Vaseline" and "lidocaine" scan connectivities in the placebo responder and NR groups (paired t-tests, $P < 0.05$). A brainstem-specific functional connectivity analysis was also conducted using the time series of the dlPFC cluster and a mask of the PAG to determine in which discrete longitudinal column dlPFC coupling was altered during placebo analgesia. Finally, after extracting parameter estimates from SUIT images representing dlPFC–PAG connectivity, linear relationships between dlPFC connectivity strength and both pain intensity ratings and dlPFC metabolite concentrations were determined (Pearson's correlations, $P < 0.05$).

For both the functional activation and connectivity analyses, the location of significant clusters in MNI space was tabulated and labeled consistent to Mai et al. (2015). For display purposes, significant clusters were overlaid onto a mean T1-weighted anatomical image of all participants.

Results

Psychophysics

Two of the participants MRI scans were excluded because of technical or data quality issues resulting in 36 participants remaining for further analysis. Twenty of the remaining 36 participants were classified as placebo responders (mean ± SEM pain intensity: control 45.82 ± 1.54, lidocaine 34.02 ± 1.91, $P < 0.001$), and the remaining 16 NR (mean ± SEM pain intensity control 41.22 ± 3.31, lidocaine 44.69 ± 3.07, $P = 0.07$). Despite differences in placebo responsivity, both responder and NR groups alike *expected* a significant pain reduction during the stimulation of the placebo "lidocaine" cream site (mean ± SEM pain intensity: responder control 49.35 ± 0.77, lidocaine 33.48 ± 1.55; NR; control 51.67 ± 1.76, lidocaine 37.14 ± 2.47; both $P < 0.001$; Fig. 1B). Additionally, neither the intensity of moderate stimuli applied during the test phase (mean ± SEM moderate temperature: responder 46.75 ± 0.05, NR 46.85 ± 0.06, $P = 0.75$) nor conditioning pain intensity ratings on both the control Vaseline and placebo lidocaine sites did not differ between placebo responders and NR (mean ± SEM pain intensity: control responder 46.52 ± 2.37, NR 42.35 ± 3.85, $P = 0.37$; lidocaine responder 28.58 ± 2.75, NR 27.45, $P = 0.82$; Supplementary Fig. 1).

Consistent with our hypothesis, placebo responders displayed greater pain rating consistency (low variability to identical noxious stimuli) than NR during the conditioning phase when low and moderate temperatures were applied to the placebo "lidocaine" and control Vaseline cream sites, respectively, as well as when moderate intensity stimuli were applied to the control site during the test phase (pain intensity SD ± SEM: conditioning control site; responders 6.66 ± 0.54, NR 10.55 ± 1.30, $P = 0.008$; conditioning "lidocaine" site; responders 8.34 ± 0.64, NR 11.98 ± 1.42, $P = 0.02$; test control site: responders 3.27 ± 0.47, NR 6.36 ± 1.01, $P = 0.008$; test "lidocaine" site: responders 4.08 ± 0.42, NR 5.10 ± 0.62, $P = 0.19$; Fig. 1C).

In all participants, a significant positive relationship was found between pain rating consistency in both the conditioning and test phases during the stimulation of the placebo "lidocaine" site ($r = 0.59$, $P < 0.001$; Fig. 1D). In addition, there was a significant negative relationship between the magnitude of placebo analgesia and pain rating consistency during the stimulation of the placebo "lidocaine" site during the conditioning phase ($r = -0.53$, $P < 0.001$; Fig. 1E). That is, greater rating consistency during conditioning was associated with greater rating consistency during the test phase on the following day, and greater rating consistency during the conditioning phase was associated with greater placebo analgesia.

Spectroscopy

A representation 1H-MRS spectra and the location of the dlPFC sampling region are shown in Fig. 2A and B. The mean tissue fraction within the dlPFC volume collected consisted of 46% gray matter, 53% white matter, and 1% CSF—and each participant's relative tissue fraction was then utilized in calculating tissue-corrected concentrations of metabolites of interest. Fractions of each tissue type and mean spectra FWHM did not demonstrate significant group-level differences (mean ± SEM gray matter: responder 0.47 ± 0.01, NR 0.44 ± 0.02, $P = 0.16$; white matter: responder 0.52 ± 0.01, NR 0.55 ± 0.02, $P = 0.19$; CSF: responder 0.01 ± 0.01, NR 0.01 ± 0.01, $P = 0.84$; FWHM: responder 9.38 ± 0.37, NR 9.94 ± 0.29, $P = 0.27$).

In contrast to our hypothesis, we identified no significant group-level differences in tissue-corrected concentration in any metabolite of interest between placebo responders and NR (mean ± SEM tissue-corrected concentration GABA: responders = 0.99 ± 0.09, NR = 0.94 ± 0.11; Glu: responders = 13.62 ± 0.19, NR = 13.24 ± 0.24; NAA: responders = 14.60 ± 0.29, NR = 14.25 ± 0.27; mINS: responders = 9.57 ± 0.16, NR = 9.46 ± 0.24; 2-sample t-test, all $P > 0.05$; Fig. 2C).

Linear regression was then conducted using the tissue-corrected concentration of each metabolite of interest and pain rating consistency during conditioning to assess whether, instead of being involved with the placebo response itself, altered dlPFC biochemistry related to an individual's ability to acquire accurate placebo associations. No significant interaction was observed in GABA, mINS, or NAA. However, a robust inverse correlation was identified between the tissue-corrected concentration of Glu and conditioning pain rating consistency on the placebo-treated site ($R = -0.41$, $P = 0.01$; Fig. 2D). That is, less variable pain rating responses during placebo-site conditioning were associated with greater concentration of dlPFC Glu.

Brain activation changes associated with pain and placebo

During pain, across all participants, signal intensity increased in the bilateral primary somatosensory cortex, bilateral insula,

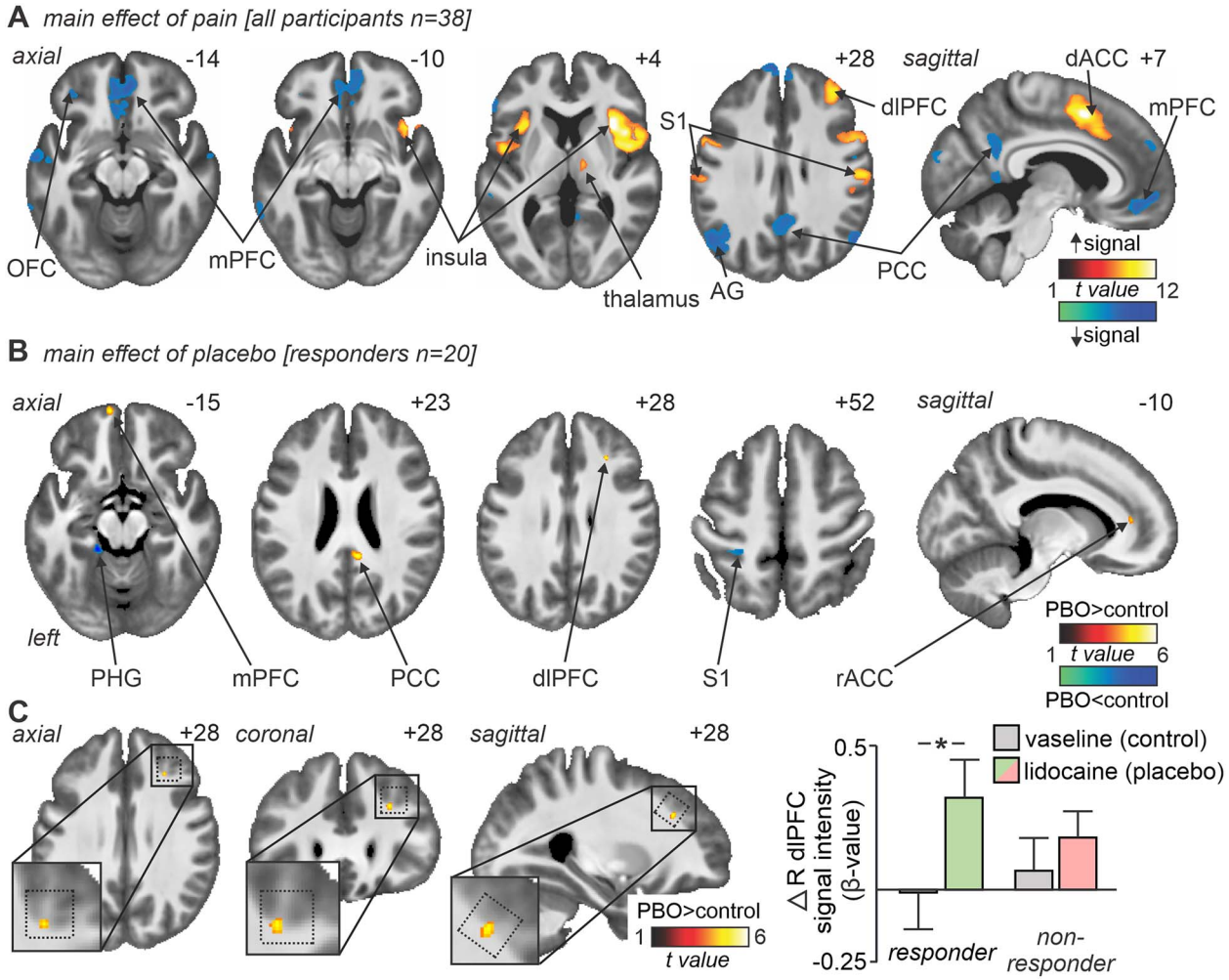

Fig. 3. Main effects of pain and placebo, biochemical and functional overlap within the right dlPFC. A) Areas in which signal intensity increased and decreased during the noxious stimulation of the control Vaseline cream site. B) Areas in which placebo responders showed significant signal intensity increases during the noxious stimulation of the "lidocaine" cream relative to during the stimulation of the control Vaseline cream site. C) Converting the mean spectroscopy cube to a volume of interest mask and applying it to the placebo main effect analysis revealed that the significant activation observed within the ipsilateral dlPFC was both within the spectroscopy volume collected, and additionally, survived multiple comparisons correction. To the right are plots of right dlPFC signal intensity change differences during noxious stimuli delivered to the control versus "lidocaine" cream sites in responder and NR groups. All clusters are overlaid onto a series of slices of a T1-weighted anatomical image set. Slice location in MNI space are indicated at the top of each slice. OFC, orbitofrontal cortex; PCC, posterior cingulate cortex; dACC, dorsal anterior cingulate cortex; S1, primary somatosensory cortex.

anterior cingulate cortex, ipsilateral thalamus, and ipsilateral dlPFC (Fig. 3A and Table 1). In addition, significant signal intensity decreases occurred in areas of the default mode network such as in the bilateral angular gyrus (AG), bilateral posterior cingulate cortex, bilateral medial prefrontal cortex (mPFC) extending into the subgenual anterior cingulate cortex, contralateral orbitofrontal cortex, and bilateral AG.

Comparison of signal intensity change in placebo responders during the stimulation of the placebo-treated relative to control-treated sites revealed altered activation in several discrete brain regions (Fig. 3B and Table 2). Regions in which an increase in signal intensity change during the stimulation of the placebo "lidocaine" cream relative to the control Vaseline cream included the rostral anterior and posterior cingulate cortices, the contralateral ventrolateral and medial prefrontal cortices, and the ipsilateral dlPFC. In both the contralateral ventrolateral and medial prefrontal cortices, signal intensity decreased during the stimulation of the control-site but did not change significantly from baseline during placebo-site stimulation. In the posterior and rostral anterior cingulate cortices, signal decreased during the stimulation of the control-site, and increased during the stimulation of the placebo-site. Uniquely, in the ipsilateral dlPFC, signal intensity increased during placebo but did not change significantly from baseline during control-site stimulation. Conversely, 2 regions demonstrated a decrease in signal intensity change during the stimulation of the placebo "lidocaine" cream relative to the control Vaseline cream—the contralateral primary somatosensory cortex and parahippocampal gyrus (PHG). Within the primary somatosensory cortex, signal change increased during the stimulation of the control Vaseline cream site and significantly decreased from baseline during placebo-site stimulation. The PHG demonstrated a different pattern of signal intensity change such signal decreased from baseline during control-site stimulation which then significantly decreased further during the stimulation of the placebo-site.

We further inspected the placebo-related signal intensity increase in the dlPFC region and identified a significant group-level difference between the stimulation of the control- and

Table 1. Main effect of pain. Cortical regions displaying significant signal intensity changes during periods of pain relative to baseline during the stimulation of the Vaseline control cream site. contra, contralateral; dACC, dorsal anterior cingulate cortex; dlPFC, dorsolateral prefrontal cortex; ipsi, ipsilateral; mPFC, medial prefrontal cortex; OFC, orbitofrontal cortex; PCC, posterior cingulate cortex; S1, primary somatosensory cortex.

	MNI coordinates						
Region name	X	Y	Z	Cluster size	t-value	Z-score	Signal change (±SEM)
Pain > baseline							
dACC	7	6	48	6,220	11.57	7.48	1.72 ± 0.18
ipsi S1	40	−4	50	16,132	9.82	6.85	2.62 ± 0.26
contra S1	−54	−24	23	924	7.96	6.04	1.17 ± 0.15
ipsi dlPFC	38	39	28	2,160	8.44	6.26	1.71 ± 0.20
ipsi insula	50	8	15	12,714	12.64	7.81	1.71 ± 0.15
contra insula	−43	10	−4	3,231	9.04	6.53	1.41 ± 0.15
ipsi thalamus	12	−19	9	479	8.16	6.13	0.60 ± 0.07
Pain < baseline							
PCC	−6	−39	37	5,207	9.2	6.59	−1.51 ± 0.19
ipsi angular gyrus	−42	−71	24	3,460	7.65	5.89	−1.75 ± 0.22
contra angular gyrus	55	−61	23	936	7.90	6.01	−1.17 ± 0.14
ipsi mPFC	6	53	−8	3,300	7.94	6.03	−0.94 ± 0.11
contra OFC	−35	29	−20	698	8.61	6.34	−0.58 ± 0.07

Table 2. Main effect of placebo. Location in Montreal Neurological Institute space (MNI), cluster size, t-value, and signal intensity changes of brain region displaying significant signal intensity changes in placebo responders ($n = 20$) during the noxious stimulation of the placebo "lidocaine" cream site relative to the control Vaseline cream site. These clusters were then saved as volume of interest masks and activation values within the same clusters extracted from placebo nonresponders ($n = 16$). contra, contralateral; dlPFC, dorsolateral prefrontal cortex; ipsi, ipsilateral; PCC, posterior cingulate cortex; rACC, rostral anterior cingulate cortex; vlPFC, ventrolateral prefrontal cortex; mPFC, medial prefrontal cortex; PHG, parahippocampal gyrus; S1, primary somatosensory cortex.

	MNI coordinates					Placebo responder ($n = 20$)		Placebo nonresponder ($n = 16$)	
Region NAME	X	Y	Z	Cluster size	t-value	Control signal change (±SEM)	Placebo signal change (±SEM)	Control signal change (±SEM)	Placebo signal change (±SEM)
Placebo > control									
ipsi dlPFC	28	28	28	43	4.08	−0.01 ± 0.13	0.32 ± 0.12	0.06 ± 0.11	0.18 ± 0.09
PCC	7	−42	24	362	4.26	−0.52 ± 0.20	0.23 ± 0.18	−0.10 ± 0.21	0.21 ± 0.14
rACC	−10	37	9	35	3.78	−0.21 ± 0.12	0.17 ± 0.10	0.04 ± 0.09	−0.20 ± 0.08
contra vlPFC	−23	59	7	99	4.20	−1.12 ± 0.33	−0.31 ± 0.31	−0.32 ± 0.31	0.05 ± 0.31
contra mPFC	−8	60	−17	146	4.36	−0.48 ± 0.14	−0.05 ± 0.14	−0.27 ± 0.19	−0.27 ± 0.09
Placebo < control									
contra PHG	−17	−37	−15	93	4.53	−0.22 ± 0.11	−0.59 ± 0.11	−0.42 ± 0.12	−0.25 ± 0.11
contra S1	−22	−37	49	97	4.16	0.18 ± 0.11	−0.20 ± 0.15	−0.17 ± 0.22	0.21 ± 0.13

placebo-treated sites. Specifically, while both groups followed similar directions of signal change, after controlling for group, only placebo responders demonstrated a significant signal intensity increase in this region (mean ± SEM activation responder: control −0.01 ± 0.13, placebo 0.32 ± 0.13, $P < 0.001$; NR: control 0.06 ± 0.11, placebo 0.18 ± 0.09, $P = 0.21$; Fig. 3C).

Altered cortico-cortical and cortico-subcortical coupling underpin placebo responses

Functional connectivity analysis revealed a number of brain regions in placebo responders in which dlPFC connectivity over the entire scan was significantly different during the stimulation of the Vaseline (control) compared with the stimulation of the lidocaine (placebo) sites (Fig. 4A and Table 3). Significantly greater dlPFC connectivity strengths during the lidocaine compared with the Vaseline cream stimulations occurred in the left dorsal anterior cingulate cortex, right superior parietal lobule, right putamen, and the right PAG. In all of these clusters, extraction of dlPFC connectivity values revealed group-level differences, i.e. connectivity strength values were significantly different between the 2 scans in the responder group only. Significantly lower dlPFC connectivity strengths during the lidocaine compared with the Vaseline cream stimulations occurred in the mPFC and left and right amygdala and again these connectivity differences were only identified within the responder group.

Given the well-described role of the PAG in placebo and the brain's descending pain control system, we further investigated the functional coupling between the dlPFC and PAG to determine its specific localization, and whether connectivity changes were related to the overall magnitude of placebo analgesia, pain rating consistency during the conditioning phase, or dlPFC biochemistry (Fig. 4B). Brainstem-specific analysis revealed that the significant PAG cluster resided primarily within the caudal lateral PAG column (lPAG) and spreading

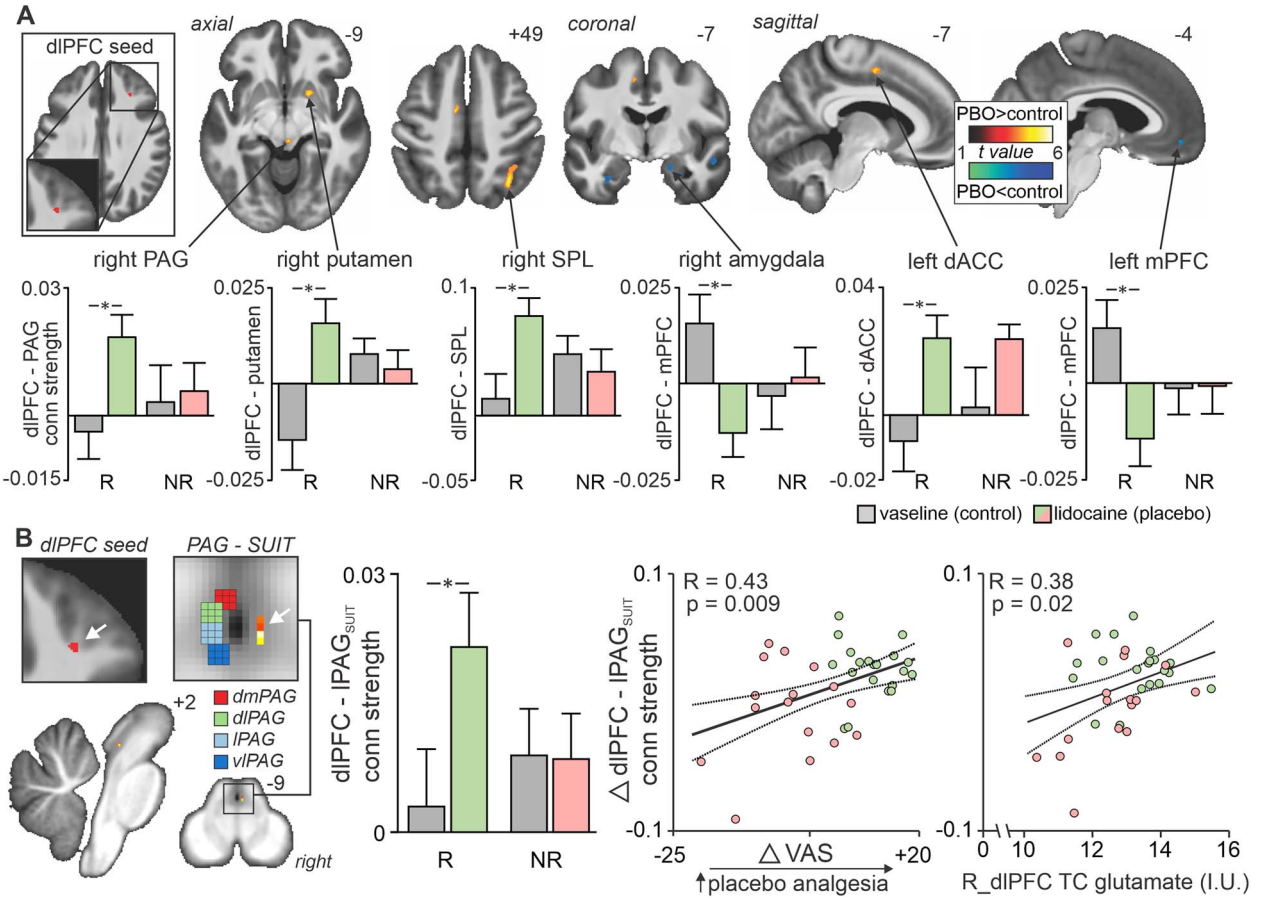

Fig. 4. Changes in functional coupling with the right dlPFC. A) Brain regions in placebo responders where functional coupling with the right dlPFC was significantly different between the stimulation of the placebo "lidocaine" treated site relative to the stimulation of the control Vaseline site. Clusters are overlaid onto an individual T1-weighted anatomical image. Slice locations in MNI space are indicated at the top of each slice. Below are plots of mean (±SEM) dlPFC connectivity strengths during the stimulation of Vaseline and lidocaine creams split between responder (R) and NR groups. *$P < 0.05$. B) Plots of connectivity strengths between the dlPFC and midbrain PAG matter against placebo analgesia, pain percept variability (pain rating consistency) during the stimulation of the placebo-treated site during the conditioning phase, and dlPFC Glu concentration. dACC, dorsal anterior cingulate cortex; SPL, superior parietal lobule.

Table 3. Right dorsolateral prefrontal cortex (dlPFC) coupling. Location in Montreal Neurological Institute space (MNI), cluster size, *t*-value, and for clusters that displayed significantly different dorsolateral prefrontal cortex (dlPFC) connectivity strength values between Vaseline and lidocaine scans. contra, contralateral; dACC, dorsal anterior cingulate cortex; ipsi, ipsilateral; mPFC, medial prefrontal cortex; lPAG, lateral midbrain periaqueductal gray matter; SPL, superior parietal lobule.

	MNI coordinates					Placebo responders dlPFC connectivity strength (mean ± SEM × 10^{-2})		Placebo nonresponders dlPFC connectivity strength (mean ± SEM × 10^{-2})	
Region	X	Y	Z	Cluster size	*t*-value	Control scan	Placebo scan	Control scan	Placebo scan
Placebo* > *control									
ipsi SPL	32	−60	49	409	4.49	1.3 ± 1.9	7.8 ± 1.4	4.8 ± 1.4	3.5 ± 1.7
ipsi dACC	−8	−5	48	187	4.66	−0.9 ± 1.1	2.6 ± 0.8	0.5 ± 1.2	2.4 ± 0.7
ipsi putamen	21	9	−10	110	4.08	−1.5 ± 0.1	1.6 ± 0.7	0.8 ± 0.4	0.4 ± 0.5
contra putamen	−17	10	−4	138	4.13	−0.5 ± 0.6	2.3 ± 0.6	1.5 ± 0.5	1.5 ± 0.6
ipsilateral lPAG	4	−30	−9	31	4.13	−0.4 ± 0.6	1.8 ± 0.5	0.3 ± 0.8	0.6 ± 0.7
Placebo* > *control (SUIT)									
ipsi lPAG	2.5	−32.5	−9.5	10	5.67	0.3 ± 0.7	2.2 ± 0.6	0.9 ± 0.6	0.8 ± 0.5
Placebo* < *control									
contra mPFC	−4	47	−12	34	3.51	2.3 ± 1.2	−2.3 ± 1.1	−0.2 ± 1.1	−0.1 ± 1.2
ipsi amygdala	20	−7	−21	114	4.24	1.5 ± 0.8	−1.3 ± 0.6	0.3 ± 0.8	0.6 ± 0.7
contra amygdala	−31	−7	−30	131	5.25	1.8 ± 0.7	−1.3 ± 0.7	0.2 ± 1.3	−0.1 ± 1.3

dorsally into the dorsolateral column. Furthermore, a robust positive correlation was identified across all participants between the change in dlPFC–lPAG coupling and the intensity of placebo analgesia ($R = 0.43$, $P = 0.009$). This indicates that this connection not only demarcates a placebo responder, but also shows a graded response in the magnitude of pain relief experienced across all participants. Change in dlPFC–lPAG coupling also positively correlated with dlPFC tissue-corrected Glu ($R = 0.38$, $P = 0.02$). In contrast, no significant interaction was observed between pain rating consistency during the conditioning phase stimulation of the placebo-treated site and dlPFC–lPAG coupling ($R = 0.03$, $P > 0.05$). That is, while greater dlPFC–lPAG connectivity was associated with both the magnitude of placebo responses and underlying dlPFC biochemistry, the strength of this connection was not directly associated with more consistent pain rating responses during conditioning phases.

Discussion

This investigation provides a multimodal assessment of the dlPFC and its role in conditioning-based placebo analgesia. Specifically, we suggest that this role encompasses acquiring strong stimulus–response relationships in conditioning required to translate positive expectations into pain relief via placebo. We first demonstrate that a more precise pain percept during conditioning is correlated with an individual's ability to express placebo analgesia, i.e. the greater the pain rating consistency the greater the subsequent placebo analgesia. Importantly, conditioning pain ratings did not differ between placebo responders and NR, suggesting that this consistency was unrelated to sensory processing or thresholds. Furthermore, we demonstrate that dlPFC biochemistry is linearly related to this pain rating consistency, i.e. the greater the pain rating consistency, the greater the dlPFC Glu levels, although not directly to the magnitude of placebo analgesia. We extended this finding to show that dlPFC activity significantly changed only in those individuals who displayed a robust placebo analgesia response. Finally, we showed that dlPFC–lPAG connectivity strength was correlated with both placebo analgesia magnitude and dlPFC Glu levels, supporting a critical role for the dlPFC to lPAG connection in placebo analgesia. Overall, our results show that there is a complex relationship between an individual's pain rating consistency, placebo analgesia, and dlPFC biochemistry, connectivity, and function.

Despite expectations of pain reduction on the placebo-treated site in all participants, only 20 of our 36 participants (55%) demonstrated significant pain modulatory responses. This proportion is consistent within the literature describing analgesic phenomena as being highly variable, only presenting in 30–50% of individuals across a population (Benedetti 1996; Petrovic et al. 2002; Youssef et al. 2016). Where our responder group demonstrated a significant reduction in perceived pain, our NR group showed a non-significant increase in perceived pain when identical intensity stimuli were applied to both the control Vaseline and placebo "lidocaine" cream sites. This increase in reported pain may represent an "uncertainty induced hyperalgesia", described previously by Yoshida et al. (2013) to relate to an individual's predictions about a future sensory input. Indeed, these predictions would be built throughout conditioning, and while expectations of pain reduction did not differ between groups, there were significant differences in pain rating consistency during the series of noxious stimuli applied to the placebo "lidocaine" cream during the conditioning and test phases. This pain rating consistency displayed intraindividual consistency, suggesting that an individual's rating consistency can be carried over between experimental phases despite the change in temperature of noxious stimulation (conditioning—low stimulus temperature and test—moderate stimulus temperature), day of testing (conditioning—day 1 and test—day 2), and surrounding environment (conditioning—outside scanner and test—inside scanner).

Consistent with our hypothesis, we found a significant relationship between pain rating consistency and placebo analgesia magnitude, i.e. the greater the rating consistency, the greater the placebo analgesia magnitude. Interestingly, while we found no significant relationship between any recorded dlPFC metabolite and placebo responsivity, there was a significant linear relationship between dlPFC Glu levels and pain rating consistency. Of course, the Glu concentration was collected at rest and represents a relatively static measurement. It may be the case that if one could measure dynamic changes in dlPFC Glu concentration, then changes in Glu concentration during noxious stimulation may indeed display a significant relationship with placebo analgesia magnitude. Moreover, our results suggest that resting dlPFC excitatory neurotransmission may underpin the variability of sensory percept (rating consistency) and may, in turn, promote placebo analgesic responses. Indeed, previous investigations have identified a role of dlPFC Glu in driving cognitive control and efficient neural processing during task performance. In both Stroop color-word conflict and 2-back counting tasks, heightened dlPFC Glu is associated with greater task performance, i.e. guiding appropriate response selection (Woodcock et al. 2018, 2019; Morgenroth et al. 2019) and it is possible that pain rating consistency is driven by this same process. It is conceivable that this dlPFC-driven rating consistency strengthens the relationship during conditioning between the conditioned stimulus and reductions in perceived pain, thereby generating greater conditioned responses in subsequent experimental phases, i.e. greater placebo analgesia.

Indeed, intracerebral Glu injections to both the hippocampus and dorsolateral striatum—sites that reciprocally project with the dlPFC in humans—accelerate response learning in experimental animals (Goodman 2020), suggesting that in humans greater resting excitatory neurotransmission may play a similar role in forming strong stimulus–response associations. Moreover, since conditioning and test phases occurred on subsequent days, and pain rating consistency between these 2 phases was linearly related, our results provide evidence that resting excitatory tone of the dlPFC may encode an individual's ability to consistently perceive and report pain responses to identical noxious stimuli.

Alongside informing response selection, the dlPFC is also known to play a critical role in maintaining and updating internal representations of goals and expectations (Cohen and Servan-Schreiber 1992; Miller and Cohen 2001). Alongside other cortical areas such as the rACC and ventrolateral prefrontal cortex, the dlPFC is part of the brain's executive-attentional network, directing our attention during the experience of sensory stimuli (Kane and Engle 2002; Curtis and D'Esposito 2003; Lorenz et al. 2003). Consistent with this, we found that placebo analgesia was associated with noxious-stimulus-evoked signal changes in these 3 brain regions. When our current experience does not match with our goals or expectations, it is thought that the dlPFC modulates regional brain activity in an attempt to match expected-experienced differentials (Roy et al. 2014; Alexander and Brown 2018; Pagnini et al. 2023).

Our analysis revealed that, during placebo, the dlPFC altered its connectivity strength with areas of the descending modulatory control network, including with the amygdala and PAG, possibly to produce this error-prediction. Preclinical and more recent

human studies have shown that the PAG can produce both pro- and antinociceptive effects (Eippert et al. 2009; Yoshida et al. 2013; Crawford et al. 2021). Specifically, as revealed through our brainstem-specific analysis, it was the lateral and dorsolateral columns of the PAG demonstrating significant coupling changes with the dlPFC. Stimulation of these 2 columns in experimental animals produces hyper-reactivity and active defensive behaviors such as flight and fight, as well as an opioid-insensitive analgesia. Additionally, we have previously demonstrated that these 2 columns are responsible for producing placebo analgesia when elicited via a response conditioning model utilizing short-lasting thermal stimuli (Crawford et al. 2021). The co-ordinates in the present investigation are remarkably similar to where we observed the greatest correlation with placebo magnitude previously, suggesting that the dlPFC may be indeed tapping into this same core brainstem circuitry. Indeed, in addition to a relationship between dlPFC Glu and pain rating consistency, we found that altered dlPFC–lPAG coupling was significantly correlated to both placebo analgesia and dlPFC Glu levels. The greater the dlPFC–lPAG coupling, the greater the excitatory tone of the dlPFC and the greater the placebo analgesia. Together, these findings support a role of the dlPFC in integrating stimulus–response associations learned through conditioning with current experience, driving error-predictive signals to match associations of pain relief by recruiting areas of the subcortex and brainstem.

Together, our results indicate that while expectation of relief alone is insufficient in activating descending pain-modulatory pathways to produce analgesia, associations learned through conditioning play a strong role in producing this phenomenon, with more precise associations between the conditioning stimulus and conditioned response leading to greater placebo analgesia that are in line with treatment expectations. How confident a participant feels a treatment will produce an expected outcome has previously been tied with mounting placebo analgesia (Grahl et al. 2018), as well as treatment response in clinical scenarios (Doyle et al. 2013; Bombard et al. 2018). It appears that pain rating consistency aids in forming a participant's stimulus–response relationships toward a placebo substance, and that the dlPFC, and in particular its connection with the PAG, plays a critical role in mediating this form of placebo analgesia.

It is important to note some limitations. First, despite the location of control Vaseline and placebo "lidocaine" creams being counterbalanced between participants, it was not possible to completely counterbalance the design such that the control cream site was always stimulated first and the placebo lidocaine second. This ordering effect could have introduced sensitization and or habituation effects, although given only approximately half of the participants displayed an analgesic response, we suggest that a significant ordering effect is unlikely. Additionally, the distribution of cream placement was similar between groups with 50% of placebo responders and 56% of placebo NR having the placebo "lidocaine" cream placed distally to the control Vaseline cream. Second, our connectivity analysis involved determining dlPFC connectivity strengths over the entire scanning period which included periods of noxious stimulation. While signal coupling may have been influenced by changes in overall signal intensity, we suggest that given the stimulus periods made up <25% of the total scan, that the effects would have been minimal, if there was any influence of stimulation at all. Third, functional analyses were threshold at $P < 0.001$, uncorrected for multiple comparisons. To reduce the chances of type II errors, we implemented a minimum cluster threshold of 20 contiguous voxels in the whole brain and 10 contiguous voxels in the brainstem-specific analysis, as well as performed small volume correction using parcels of the HCPex atlas on resulting clusters. Furthermore, dlPFC placebo-related activation survived family-wise error correction for multiple comparisons. Finally, our investigation included relatively young healthy adults (mean age 25 years; range 20–37 years) and there is evidence that brain regions such as the ACC display Glu concentration decreases with age and this decrease may be sex related (Hädel et al. 2013). While we do not know if similar changes occur in the dlPFC, it would be of interest in future investigations to widen the age range considerably and assess the potential interactions between age, dlPFC metabolite concentration, pain rating consistency, and placebo analgesia responsivity.

Conclusions

By combining ^{1}H-MRS and fMRI, this investigation demonstrates how dlPFC biochemical composition and functional connectivity may provide a route for translating associations learned through conditioning to endogenous pain relief. We provide evidence that conditioning pain rating consistency plays a profound role in generating greater analgesic effects, and further provide evidence that this rating consistency may be underpinned by basal excitatory neurotransmission in the dlPFC.

Acknowledgments

The authors acknowledge the facilities, scientific and technical assistance from the National Imaging Facility, a National Collaborative Research Infrastructure Strategy capability, at the Melbourne Brain Centre Imaging Unit, The University of Melbourne. This work was supported by a research collaboration agreement with Siemens Healthineers. The MRS sequence was developed by Edward J. Auerbach and Malgorzata Marjanska and provided by the University of Minnesota under a C2P agreement. Any questions or requests can be made directly to the corresponding author: LAH | lukeh@anatomy.usyd.edu.au

Author contributions

Lewis S. Crawford (Conceptualization, Data curation, Formal analysis, Writing—original draft, Writing—review & editing), Emily P. Mills (Conceptualization, Data curation, Writing—review & editing), A. Peek (Formal analysis, Writing—review & editing), V.G. Macefield (Conceptualization, Data curation, Writing—review & editing), K.A. Keay (Conceptualization, Resources, Writing—review & editing), and Luke A. Henderson (Conceptualization, Data curation, Funding acquisition, Writing—review & editing)

Supplementary material

Supplementary material is available at *Cerebral Cortex* online.

Funding

The Australian National Health and Medical Research Council (Grant ID 1130280).

Conflict of interest statement: None declared.

Data availability

All de-identified single participant functional data, as well as activation and connectivity contrast maps, are available from the corresponding author upon reasonable request.

Code availability

The analysis methods and software used in this article are all either open source—for instance Osprey (https://schorschinho.github.io/osprey/), or are enabled in SPM12's standard installation. For this manuscript, MATLAB version R2022b was used. No new methods or algorithms have been generated.

References

Alexander WH, Brown JW. Frontal cortex function as derived from hierarchical predictive coding. *Sci Rep*. 2018:8:3843.

Amanzio M, Benedetti F. Neuropharmacological dissection of placebo analgesia: expectation-activated opioid systems versus conditioning-activated specific subsystems. *J Neurosci*. 1999:19:484–494.

Ashar YK, Chang LJ, Wager TD. Brain mechanisms of the placebo effect: an affective appraisal account. *Annu Rev Clin Psychol*. 2017:13:73–98.

Benedetti F. The opposite effects of the opiate antagonist naloxone and the cholecystokinin antagonist proglumide on placebo analgesia. *Pain*. 1996:64:535–543.

Bombard Y, Baker GR, Orlando E, Fancott C, Bhatia P, Casalino S, Onate K, Denis J-L, Pomey M-P. Engaging patients to improve quality of care: a systematic review. *Implement Sci*. 2018:13:98.

Büchel C, Geuter S, Sprenger C, Eippert F. Placebo analgesia: a predictive coding perspective. *Neuron*. 2014:81:1223–1239.

Cohen JD, Servan-Schreiber D. Context, cortex, and dopamine: a connectionist approach to behavior and biology in schizophrenia. *Psychol Rev*. 1992:99:45–77.

Colloca L. How do placebo effects and patient-clinician relationships influence behaviors and clinical outcomes? *Pain Rep*. 2019:4:e758.

Colloca L, Benedetti F. How prior experience shapes placebo analgesia. *Pain*. 2006:124:126–133.

Colloca DL, Petrovic DP, Wager DT, Ingvar DM, Benedetti DF. How the number of learning trials affects placebo and nocebo responses. *Pain*. 2010:151:430–439.

Crawford LS, Mills EP, Hanson T, Macey PM, Glarin R, Macefield VG, Keay KA, Henderson LA. Brainstem mechanisms of pain modulation: a within-subjects 7T fMRI study of placebo analgesic and nocebo hyperalgesic responses. *J Neurosci*. 2021:41:9794–9806.

Crawford L, Mills E, Meylakh N, Macey PM, Macefield VG, Henderson LA. Brain activity changes associated with pain perception variability. *Cereb Cortex*. 2023:33(7):4145–4155.

Curtis CE, D'Esposito M. Persistent activity in the prefrontal cortex during working memory. *Trends Cogn Sci*. 2003:7:415–423.

Diedrichsen J. A spatially unbiased atlas template of the human cerebellum. *NeuroImage*. 2006:33:127–138.

Doyle C, Lennox L, Bell D. A systematic review of evidence on the links between patient experience and clinical safety and effectiveness. *BMJ Open*. 2013:3:e001570.

Eippert F, Bingel U, Schoell ED, Yacubian J, Klinger R, Lorenz J, Büchel C. Activation of the opioidergic descending pain control system underlies placebo analgesia. *Neuron*. 2009:63:533–543.

Faul F, Erdfelder E, Lang AG, Buchner A. G*power 3: a flexible statistical power analysis program for the social, behavioral, and biomedical sciences. *Behav Res Methods*. 2007:39:175–191.

Goodman J. Place vs. response learning: history, controversy, and neurobiology. *Front Behav Neurosci*. 2020:14:598570.

Grachev ID, Fredrickson BE, Apkarian VA. Abnormal brain chemistry in chronic back pain: an in vivo proton magnetic resonance spectroscopy study. *Pain*. 2000:89:7–18.

Grachev ID, Thomas PS, Ramachandran TS. Decreased levels of N-acetylaspartate in dorsolateral prefrontal cortex in a case of intractable severe sympathetically mediated chronic pain (complex regional pain syndrome, type I). *Brain Cogn*. 2002:49:102–113.

Grahl A, Onat S, Büchel C. The periaqueductal gray and Bayesian integration in placebo analgesia. *eLife*. 2018:7.

Gussew A, Rzanny R, Güllmar D, Scholle HC, Reichenbach JR. 1H-MR spectroscopic detection of metabolic changes in pain processing brain regions in the presence of non-specific chronic low back pain. *NeuroImage*. 2011:54:1315–1323.

Hädel S, Wirth C, Rapp M, Gallinat J, Schubert F. Effects of age and sex on the concentrations of glutamate and glutamine in the human brain. *J Magn Reson Imaging*. 2013:38:1480–1487.

Harris AD, Puts NAJ, Barker PB, Edden RAE. Spectral-editing measurements of GABA in the human brain with and without macromolecule suppression. *Magn Reson Med*. 2015:74:1523–1529.

Hassel B, Dingledine R. Chapter 17 - glutamate and glutamate receptors. In: Brady ST, Siegel GJ, Albers RW, Price DL, editors. *Basic neurochemistry*. 8th ed. New York (NY): Academic Press; 2012. pp. 342–366

Henderson LA, Di Pietro F, Youssef AM, Lee S, Tam S, Akhter R, Mills EP, Murray GM, Peck CC, Macey PM. Effect of expectation on pain processing: a psychophysics and functional MRI analysis. *Front Neurosci*. 2020:14:6–6.

Hibi D, Takamoto K, Iwama Y, Ebina S, Nishimaru H, Matsumoto J, Takamura Y, Yamazaki M, Nishijo H. Impaired hemodynamic activity in the right dorsolateral prefrontal cortex is associated with impairment of placebo analgesia and clinical symptoms in postherpetic neuralgia. *IBRO Rep*. 2020:8:56–64.

Huang CC, Rolls ET, Feng J, Lin CP. An extended human connectome project multimodal parcellation atlas of the human cortex and subcortical areas. *Brain Struct Funct*. 2022:227:763–778.

Kane MJ, Engle RW. The role of prefrontal cortex in working-memory capacity, executive attention, and general fluid intelligence: an individual-differences perspective. *Psychon Bull Rev*. 2002:9:637–671.

Kaptchuk TJ, Shaw J, Kerr CE, Conboy LA, Kelley JM, Csordas TJ, Lembo AJ, Jacobson EE. "Maybe I made up the whole thing": placebos and patients' experiences in a randomized controlled trial. *Cult Med Psychiatry*. 2009:33:382–411.

Kong J, Kaptchuk TJ, Polich G, Kirsch I, Vangel M, Zyloney C, Rosen B, Gollub R. Expectancy and treatment interactions: a dissociation between acupuncture analgesia and expectancy evoked placebo analgesia. *NeuroImage*. 2009:45:940–949.

Krummenacher P, Candia V, Folkers G, Schedlowski M, Schönbächler G. Prefrontal cortex modulates placebo analgesia. *Pain*. 2010:148:368–374.

Lorenz J, Minoshima S, Casey KL. Keeping pain out of mind: the role of the dorsolateral prefrontal cortex in pain modulation. *Brain*. 2003:126:1079–1091.

Mai JK, Majtanik M, Paxinos G. *Atlas of the human brain*. Cambridge, Massachusetts: Academic Press; 2015

Medoff ZM, Colloca L. Placebo analgesia: understanding the mechanisms. *Pain Manag*. 2015:5:89–96.

Miller EK, Cohen JD. An integrative theory of prefrontal cortex function. *Annu Rev Neurosci*. 2001:24:167–202.

Mills EP, Alshelh Z, Kosanovic D, Di Pietro F, Vickers ER, Macey PM, Henderson LA. Altered brainstem pain-modulation circuitry connectivity during spontaneous pain intensity fluctuations. *J Pain Res*. 2020:13:2223–2235.

Morgenroth E, Orlov N, Lythgoe DJ, Stone JM, Barker H, Munro J, Eysenck M, Allen P. Altered relationship between prefrontal

glutamate and activation during cognitive control in people with high trait anxiety. *Cortex*. 2019:117:53–63.

Mylius V, Ayache SS, Ahdab R, Farhat WH, Zouari HG, Belke M, Brugières P, Wehrmann E, Krakow K, Timmesfeld N, et al. Definition of DLPFC and M1 according to anatomical landmarks for navigated brain stimulation: inter-rater reliability, accuracy, and influence of gender and age. *NeuroImage*. 2013:78:224–232.

Oeltzschner G, Zöllner HJ, Hui SCN, Mikkelsen M, Saleh MG, Tapper S, Edden RAE. Osprey: open-source processing, reconstruction & estimation of magnetic resonance spectroscopy data. *J Neurosci Methods*. 2020:343:108827.

Pagnini F, Barbiani D, Cavalera C, Volpato E, Grosso F, Minazzi GA, Vailati Riboni F, Graziano F, Di Tella S, Manzoni GM, et al. Placebo and nocebo effects as Bayesian-brain phenomena: the overlooked role of likelihood and attention. *Perspect Psychol Sci*. 2023:17456916221141383.

Parry E, Ogollah R, Peat G. Significant pain variability in persons with, or at high risk of, knee osteoarthritis: preliminary investigation based on secondary analysis of cohort data. *BMC Musculoskelet Disord*. 2017:18:80.

Peek AL, Rebbeck T, Puts NAJ, Watson J, Aguila M-ER, Leaver AM. Brain GABA and glutamate levels across pain conditions: a systematic literature review and meta-analysis of 1H-MRS studies using the MRS-Q quality assessment tool. *NeuroImage*. 2020:210:116532.

Penny WD, Friston KJ, Ashburner JT, Kiebel SJ, Nichols TE, editors. *Statistical parametric mapping: the analysis of functional brain images*. Elsevier; 2011.

Petrovic P, Kalso E, Petersson KM, Ingvar M. Placebo and opioid analgesia–imaging a shared neuronal network. *Science*. 2002:295:1737.

Provencher SW. Estimation of metabolite concentrations from localized in vivo proton NMR spectra. *Magn Reson Med*. 1993:30: 672–679.

Rosenbloom MH, Schmahmann JD, Price BH. The functional neuroanatomy of decision-making. *J Neuropsychiatry Clin Neurosci*. 2012:24:266–277.

Roy M, Shohamy D, Daw N, Jepma M, Wimmer GE, Wager TD. Representation of aversive prediction errors in the human periaqueductal gray. *Nat Neurosci*. 2014:17:1607–1612.

Särkkä S, Solin A, Nummenmaa A, Vehtari A, Auranen T, Vanni S, Lin F-H. Dynamic retrospective filtering of physiological noise in BOLD fMRI: DRIFTER. *NeuroImage*. 2012:60(2): 1517–1527.

Schenk LA, Colloca L. The neural processes of acquiring placebo effects through observation. *NeuroImage*. 2020:209: 116510.

Sevel LS, Craggs JG, Price DD, Staud R, Robinson ME. Placebo analgesia enhances descending pain-related effective connectivity: a dynamic causal modeling study of endogenous pain modulation. *J Pain*. 2015:16:760–768.

Swift ML. GraphPad prism, data analysis, and scientific graphing. *J Chem Inf Comput Sci*. 1997:37:411–412.

Tu Y, Wilson G, Camprodon J, Dougherty DD, Vangel M, Benedetti F, Kaptchuk TJ, Gollub RL, Kong J. Manipulating placebo analgesia and nocebo hyperalgesia by changing brain excitability. *Proc Natl Acad Sci U S A*. 2021:118(19):e2101273118.

Wager TD, Rilling JK, Smith EE, Sokolik A, Casey KL, Davidson RJ, Kosslyn SM, Rose RM, Cohen JD. Placebo-induced changes in FMRI in the anticipation and experience of pain. *Science*. 2004:303: 1162–1167.

Woo C-W, Krishnan A, Wager TD. Cluster-extent based thresholding in fMRI analyses: pitfalls and recommendations. *NeuroImage*. 2014:91:412–419.

Woodcock EA, Anand C, Khatib D, Diwadkar VA, Stanley JA. Working memory modulates glutamate levels in the dorsolateral prefrontal cortex during (1)H fMRS. *Front Psychiatry*. 2018: 9:66.

Woodcock EA, Greenwald MK, Khatib D, Diwadkar VA, Stanley JA. Pharmacological stress impairs working memory performance and attenuates dorsolateral prefrontal cortex glutamate modulation. *NeuroImage*. 2019:186:437–445.

Yoshida W, Seymour B, Koltzenburg M, Dolan RJ. Uncertainty increases pain: evidence for a novel mechanism of pain modulation involving the periaqueductal gray. *J Neurosci*. 2013:33: 5638–5646.

Youssef AM, Macefield VG, Henderson LA. Cortical influences on brainstem circuitry responsible for conditioned pain modulation in humans. *Hum Brain Mapp*. 2016:37:2630–2644.